RAB8B Is Required for Activity and Caveolar Endocytosis of LRP6

Kubilay Demir,[1] Nadine Kirsch,[2] Carlo A. Beretta,[1] Gerrit Erdmann,[1] Dierk Ingelfinger,[1] Enrico Moro,[3] Francesco Argenton,[4] Matthias Carl,[1] Christof Niehrs,[2,5] and Michael Boutros[1,*]
[1]German Cancer Research Center (DKFZ), Division of Signaling and Functional Genomics, Heidelberg University, Department of Cell and Molecular Biology, Medical Faculty Mannheim, 69120 Heidelberg, Germany
[2]German Cancer Research Center (DKFZ), Division of Molecular Embryology, 69120 Heidelberg, Germany
[3]Department of Biomedical Sciences, University of Padova, 35131 Padova, Italy
[4]Department of Biology, University of Padova, 35131 Padova, Italy
[5]Institute of Molecular Biology, 55128 Mainz, Germany
*Correspondence: m.boutros@dkfz.de
http://dx.doi.org/10.1016/j.celrep.2013.08.008

SUMMARY

Wnt/β-catenin signaling plays an important role in embryonic development and adult tissue homeostasis. When Wnt ligands bind to the receptor complex, LRP5/6 coreceptors are activated by phosphorylation and concomitantly endocytosed. In vertebrates, Wnt ligands induce caveolin-dependent endocytosis of LRP6 to relay signal downstream, whereas antagonists such as Dickkopf promote clathrin-dependent endocytosis, leading to inhibition. However, little is known about how LRP6 is directed to different internalization mechanisms, and how caveolin-dependent endocytosis is mediated. In an RNAi screen, we identified the Rab GTPase RAB8B as being required for Wnt/β-catenin signaling. RAB8B depletion reduces LRP6 activity, β-catenin accumulation, and induction of Wnt target genes, whereas RAB8B overexpression promotes LRP6 activity and internalization and rescues inhibition of caveolar endocytosis. In *Xenopus laevis* and *Danio rerio*, RAB8B morphants show lower Wnt activity during embryonic development. Our results implicate RAB8B as an essential evolutionary conserved component of Wnt/β-catenin signaling through regulation of LRP6 activity and endocytosis.

INTRODUCTION

The Wnt protein family regulates embryonic development including cell polarity and proliferation, tissue specification, and axis patterning (reviewed in Klaus and Birchmeier, 2008). Dysregulation of Wnt pathway activity has been implicated in human disorders and cancer (reviewed in MacDonald et al., 2009). The Wnt/β-catenin pathway is initiated by binding of

Wnt to the Fz receptor complex through recruiting multidomain protein Dvl to the plasma membrane (Bilic et al., 2007). This facilitates establishment of signalosomes, which includes the scaffolding protein Axin, GSK3β, and CK1γ kinases and, in turn, leads to dual-phosphorylation of LRP6 (Davidson et al., 2005; Zeng et al., 2005). Signalosome formation induces internalization of the receptor complex through a caveolin-dependent process (Yamamoto et al., 2006). Subsequently, endocytosed vesicles fuse with early endosomes and mature into multivesicular bodies (MVBs) by the ESCRT complex (Taelman et al., 2010). Sequestration of GSK3β into MVBs inactivates the β-catenin destruction complex, allowing the accumulation of active β-catenin in the nucleus where it interacts with T cell factor and lymphoid enhancer factor (TCF/LEF) complex (Behrens et al., 1996).

Rabs are small GTP binding proteins of the Ras GTPase superfamily that regulate intracellular vesicular trafficking between membrane-enclosed compartments in eukaryotic cells (reviewed in Stenmark, 2009). Many of the more than 60 different Rab proteins encoded in the human genome have been linked to signaling pathways including Hedgehog, EGF, and Notch signaling pathways (Emery et al., 2005; Evans et al., 2003; Miaczynska et al., 2004). The housekeeping endocytic Rabs, such as Rab5, Rab11, and Rab7, are also involved in endocytosis, recycling, and degradation of LRP6, respectively (Sakane et al., 2010).

Here, we provide evidence that RAB8B is a positive regulator of Wnt/β-catenin signaling at the level of receptor activity and internalization in ligand-receiving cells. RAB8B depletion specifically reduces Wnt activity, without an effect on other major signaling pathways. Furthermore, RAB8B synergizes with LRP6 in a Wnt and Dvl-dependent manner. RAB8B interacts and colocalizes with LRP6 and its activator CK1γ at the plasma membrane. Dvl1 recruits RAB8B in Dvl puncta, and Wnt3a induces RAB8B's interaction with its activator RABIN8. RAB8B promotes activity and internalization of LRP6 and rescues caveolar inhibition of LRP6 endocytosis. Furthermore, RAB8B is also required for Wnt activity during vertebrate development and the regulation of Wnt target genes.
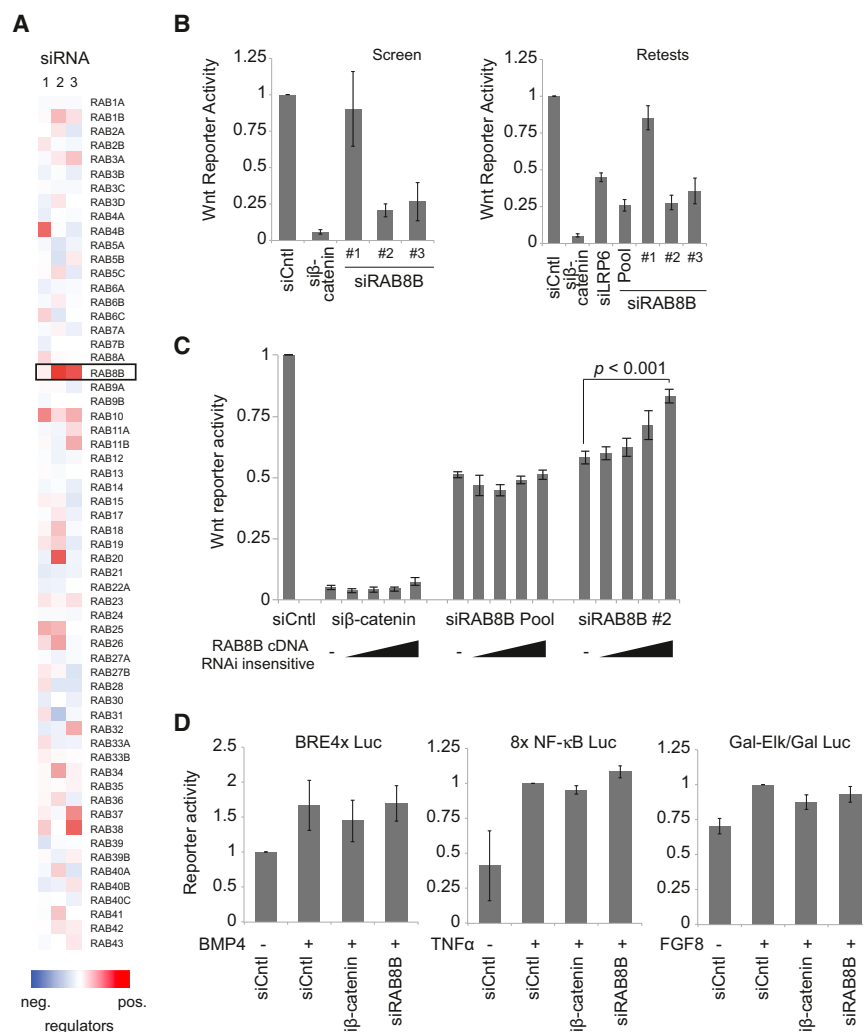
Figure 1. An RNAi Screen Identified *RAB8B* as a Positive Regulator of Wnt/β-catenin Pathway

(A) *RAB8B* ranked the top-scoring candidate in the Rab GTPase family. Heatmap displaying individual siRNA *Z* scores in HCT116.

(B) Wnt reporter assay showing percent of control (POC) normalized relative luminescence unit (RLU) screen scores of RAB8B siRNAs, and their confirmation in HCT116.

(C) Human RAB8B-RNAi-insensitive expression construct, harboring silent mutations in the siRNA#2 complementary region, rescued siRNA#2 phenotype but failed to rescue the pool that also contains targeting siRNAs #1 and #3 (HEK 293T).

(D) RAB8B depletion did not reduce the activity of other major pathway reporters, including BMP/Smad1- BREX4-luc (induced by BMP4), TNF-α/NFκB - 8 × NFκB-luc (induced by TNF-α), Ras/ERK - Gal-Elk/Gal-luc (induced by FGF8). Assays were performed in HEK 293T cells. All reporter assays were performed as three replicates (n = 3), and error bars represent ±SD.

See also Figures S1 and S2.

RESULTS

An RNAi Screen Identifies *RAB8B* as a Regulator of Canonical Wnt Signaling

In order to identify factors that regulate trafficking of Wnt pathway components, we performed an RNAi screen using a modified β-catenin/TCF reporter (Figures S1A–S1C). RAB8B was identified as a strong positive regulator of the pathway among other Rabs (Figure 1A). Individual RAB8B small interfering RNAs (siRNAs) reduced Wnt reporter activity up to 4-fold, and they were further retested in different cell lines (Figures 1B, S1D, and S1E). We then assessed the specificity of the knockdown by rescue experiments with an RNAi-insensitive RAB8B expression construct. Although the RNAi-insensitive complementary DNA (cDNA) rescued the knockdown phenotype (Figure 1C), a wild-type construct did not (Figure S1F). Furthermore, a constitutively active RNAi-insensitive RAB8B construct fully rescued RNAi phenotype and even further activated the pathway (Figure S1G). We also verified the RNAi insensitivity at the protein level (Figure S1H).

To investigate whether RAB8B knockdown also affected other signaling pathways, we tested a panel of signaling reporters monitoring BMP/Smad1, tumor necrosis factor (TNF)-α/NFκB, Ras/ERK, JAK/STAT3, and transforming growth factor (TGF)-β/Smad2 pathway activities (Figures 1D and S1I). These experiments showed that, in contrast to its effects on the Wnt pathway, RAB8B depletion did not impair the activity of these pathways. RAB8B depletion also did not affect cell viability (Figure S1J).

The human genome encodes two RAB8 isoforms, RAB8A and RAB8B, that share 40% amino acid identity in the C-terminal variable region. RAB8A silencing weakly reduced Wnt reporter activity but had no effect on the expression of endogenous target genes (Figures S2A–S2C), suggesting they have different biological functions. Taken together, these results suggest that RAB8B is required for Wnt signal transduction, whereas other major signaling pathways do not appear to require its function.

RAB8B Is Required at the Level of Receptors in Wnt-Receiving Cells

To epistatically map RAB8B's function in the Wnt pathway, we depleted RAB8B in human embryonic kidney (HEK) 293T cells and stimulated the pathway at different levels. RAB8B knockdown reduced Wnt reporter activity induced by Wnt3a or expression of Dvl1, but not when constitutively active LRP6Δe1-4 was expressed (Figure 2A). This result points toward a function for RAB8B at the receptor level in Wnt-receiving cells. Consistently, RAB8B depletion also reduced reporter activity in cells expressing Wnt3a but not those expressing β-catenin (Figure S2D).

A

B

C
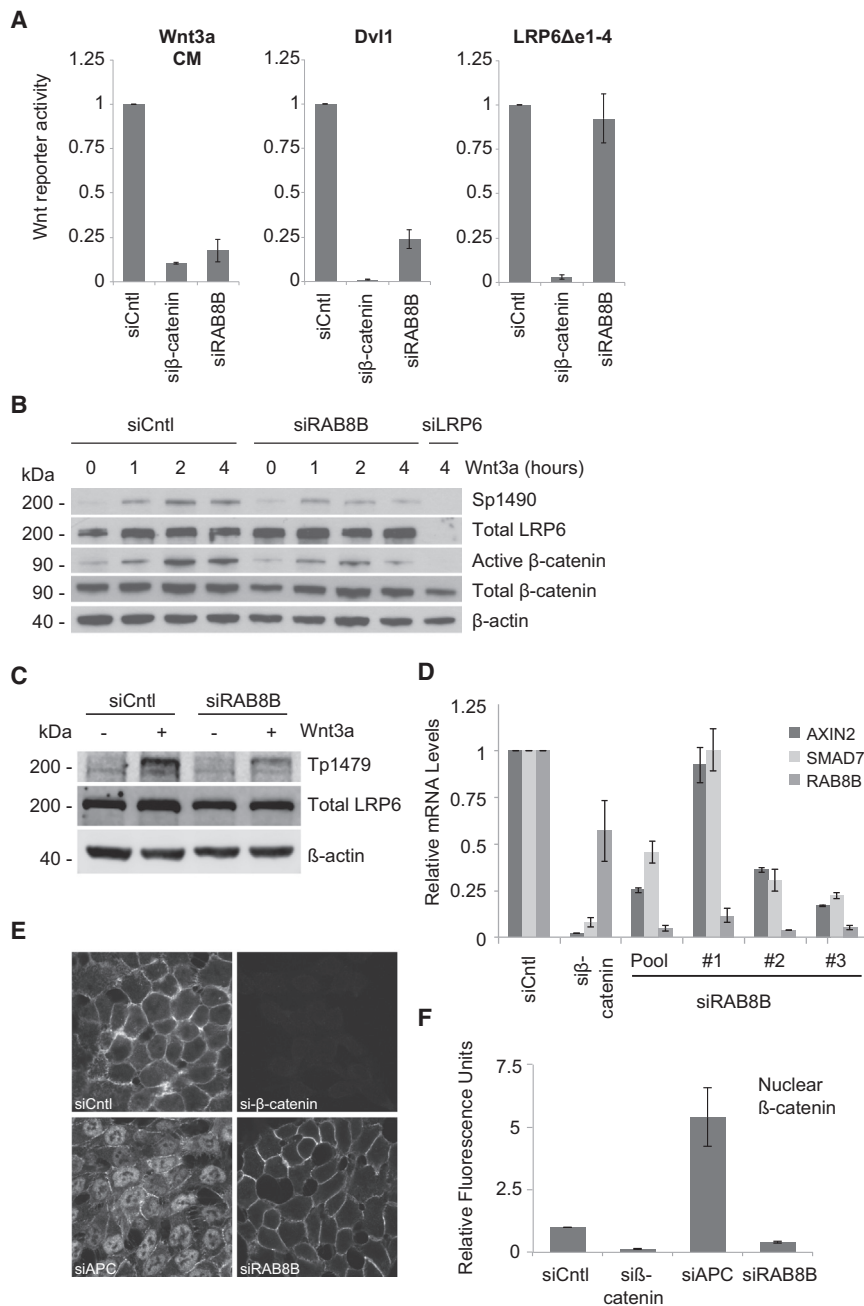

D

E

F

Figure 2. RAB8B's Function Was Required at the Level of Receptors in the Wnt-Receiving Cell

(A) RAB8B depletion reduced Wnt reporter activity when activated with Wnt3a conditioned medium (Wnt3a CM) and Dvl1 but not constitutively active LRP6Δe1-4 coexpression in HEK 293T cells.

(B) RAB8B knockdown reduced Wnt3a-induced active LRP6 (Sp1490/GSK3β phosphorylation site) and β-catenin levels, whereas total protein levels remained unchanged in HEK 293T cells.

(C) RAB8B depletion reduced signalosome formation as detected by lower LRP6 phosphorylation (Tp1479/CK1γ) after 1.5 hr of Wnt3a exposure in HEK 293T.

(D) Wnt target genes AXIN2 and SMAD7 mRNA levels were reduced in cells that were depleted for RAB8B (HCT116).

(E) RAB8B knockdown cells had lower nuclear β-catenin, whereas depletion of destruction complex member APC resulted in increased accumulation in HCT116.

(F) Relative quantification of nuclear ß-catenin levels of the images in Figure 2E.

Error bars represent ±SD of three replicates. See also Figure S2.

S2G). Next, we asked whether β-catenin nuclear translocation was perturbed in RAB8B knockdown that could have reduced the Wnt transcriptional activity. RAB8B depletion decreased nuclear β-catenin levels underscoring its requirement upstream of β-catenin (Figures 2E, 2F, S2H, and S2I). Together, these results demonstrate that RAB8B depletion reduces endogenous Wnt signaling activity, and that RAB8B is required at the level of LRP6 in Wnt-receiving cells.

RAB8B Is Activated by Wnt3a and Relocated by Dvl1 to Promote LRP6 Activity

We then investigated whether increasing RAB8B activity could stimulate Wnt pathway activity. Therefore, we generated constitutively active (c.a., Q67L) and dominant-negative (d.n., T22N) forms of RAB8B (Hattula et al., 2002) and expressed them in HEK 293T cells together with LRP6. RAB8B c.a., but not RAB8B d.n., acted synergistically with LRP6 on Wnt pathway activity, which was also found with a c.a. form of *Xenopus* RAB8B (Figures 3A and S3A). We did not observe a synergistic activity with RAB8B wild-type (WT), indicating that the wild-type protein might require activation by a Rab GEF protein (Figure S3B). In the presence of Wnt3a stimulation, RAB8B-WT synergized with LRP6 (Figure 3B). Furthermore, increased levels of active LRP6 and β-catenin in RAB8B-WT-expressing cells were observed in Wnt3a-stimulated cells (Figure 3C). These observations implicate a

Phosphorylations of the intracellular domain of LRP6 by CK1γ and GSK3β are hallmarks of Wnt signalosome formation, resulting in the stabilization of transcriptionally active β-catenin. Therefore, we tested whether RAB8B has an effect on receptor activity and subsequent stabilization of β-catenin. In accordance with the epistasis analysis, RAB8B silencing reduced signalosome formation by reducing GSK3β- and CK1γ-mediated LRP6 phosphorylation, and active β-catenin levels, whereas total LRP6 and β-catenin levels remained unchanged (Figures 2B and 2C). In RAB8B-depleted cells, mRNA levels of the Wnt target genes AXIN2 and SMAD7 were reduced (Figures 2D and S2E–
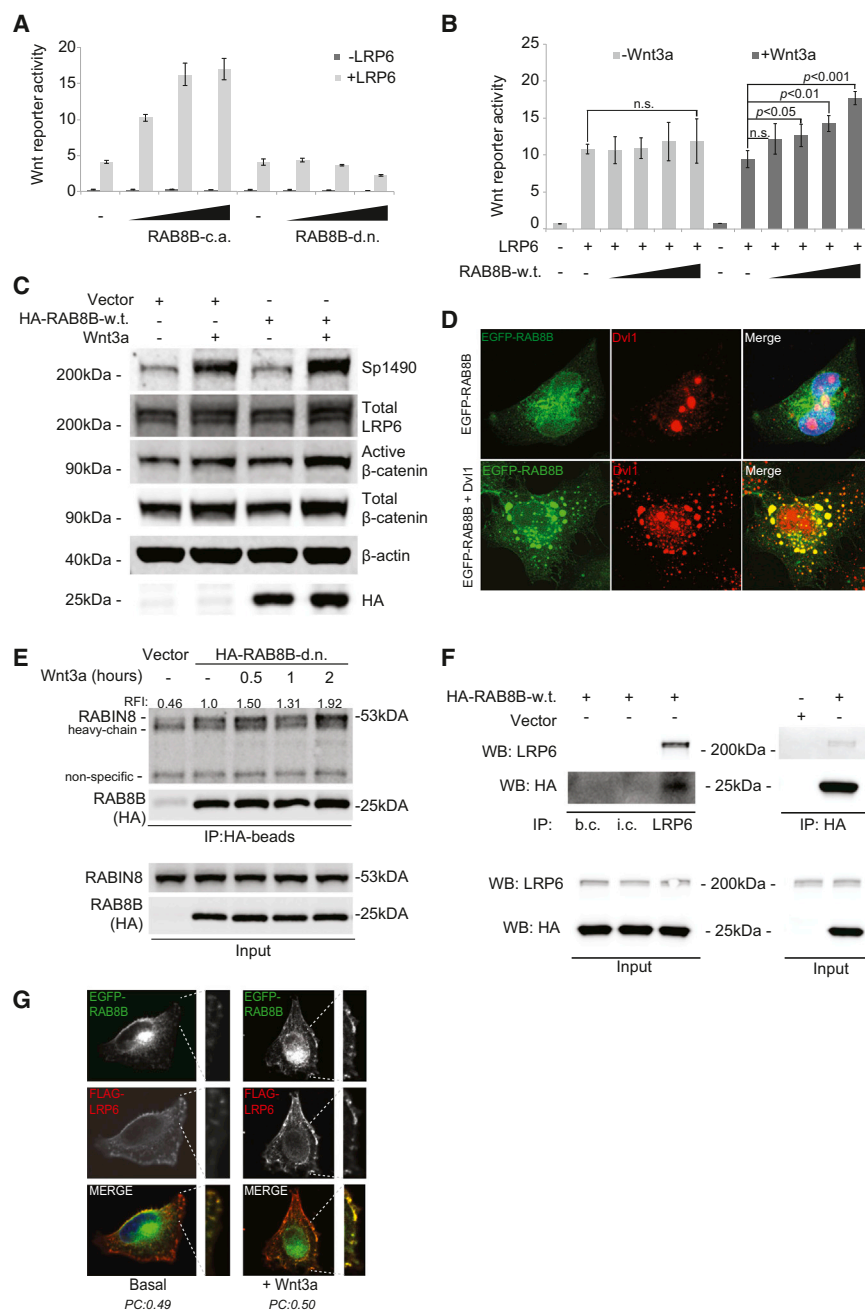
Figure 3. RAB8B Is Activated by Wnt Ligands and Relocalized by Dvl1 to Promote LRP6 Activity

(A) In the Wnt reporter assay, LRP6 synergized with coexpression of constitutively active mutant (c.a., Q67L), whereas dominant-negative mutant (d.n., T22N) had an inhibitory affect (HEK 293T).

(B) In the same assay, RAB8B-WT synergized with LRP6 only in the presence of recombinant Wnt3a in HEK 293T (n.s., not significant).

(C) RAB8B-WT expression increased active LRP6 and β-catenin levels in the presence of recombinant Wnt3a after 2 hr in HEK 293T.

(D) Dvl1 coexpression recruited RAB8B in Dvl1 puncta (HeLa).

(E) RAB8B interaction with its activator RABIN8 is stimulated by adding recombinant Wnt3a (normalized to nonspecific band; RFI. relative fluorescence intensity) in HEK 293T.

(F and G) RAB8B-WT coimmunoprecipitated with endogenous LRP6 (HEK 293T; b.c., bead control; i.c., isotype control), and both proteins colocalized at the plasma membrane that was further promoted by adding recombinant Wnt3a (1 hr) (PC, Pearson's coefficient) (HeLa).

Error bars represent ±SD of three replicates. See also Figures S3 and S4.

Dvl1 puncta (Figures 3D and S3E–S3G), which are also endosomal PI3P marker positive (Taelman et al., 2010). Furthermore, we observed a Wnt-ligand-dependent stimulation of RAB8B interaction with its activator guanine exchange factor protein RABIN8 (Hattula et al., 2002) (Figure 3E). These observations showed that Wnt ligands and Dvl regulate RAB8B's activity and trafficking function. In accordance, RAB8B depletion had no effect on Wnt signaling when the pathway was activated through self-aggregating LRP6Δe1-4, which recruits Axin independent of upstream signaling (Figure 2A). Furthermore, RAB8B knockdown cells had also lower Wnt reporter activity when pathway was stimulated with wild-type LRP6, which could be rescued by coexpression of its activator CK1γ (Figure S3H). All together, these results impli-

Wnt-dependent activation of RAB8B. These findings were further supported by experiments in Wnt-expressing HCT116 cells where RAB8B-c.a. alone readily increased pathway activity, whereas higher amounts of WT RAB8B were required to achieve the same degree of reporter induction (Figure S3C).

We then tested whether we could promote RAB8B-WT activity by coexpressing Wnt/β-catenin pathway activator Dvl1. RAB8B-WT displayed a dose-dependent synergistic activity when coexpressed with Dvl1 (Figure S3D). Then, we checked whether Dvl1 had an affect on RAB8B's subcellular localization. Dvl1 coexpression induced strong RAB8B accumulation within large

cate that RAB8B functions at the level of signalosome formation and promotes LRP6 activity.

Next, we investigated the mechanistic basis of the observed synergy of RAB8B and LRP6. Coimmunoprecipitation (Co-IP) experiments revealed an interaction between endogenous LRP6 and HA-RAB8B (Figure 3F), but not with a control transmembrane protein FLRT3 (Figure S3I). In accordance, EGFP-RAB8B and FLAG-LRP6 epitope-tagged proteins colocalized at the plasma membrane, which could be further promoted by addition of recombinant Wnt3a (Figure 3G). Furthermore, RAB8B also interacts with signalosome component CK1γ

A

Vector | RAB8B-c.a. | RAB8B-d.n.

Wnt3a (hours): 0 0.5 1 2 | 0 0.5 1 2 | 0 0.5 1 2

RFI: 1.0 1.25 0.67 0.52 | 0.44 0.51 0.64 0.73 | 1.25 0.94 1.07 1.23

IP: FLAG — WB: Biotin (surface) — -200kDA

IP: FLAG — WB: FLAG (total) — -200kDA

B

siCntl | siRAB8B

Wnt3a (hours): - 1 2 | - 1 2

RFI: 1.0 0.94 0.61 | 1.0 0.93 0.96

IP: FLAG — WB: Biotin (surface) — -200kDA

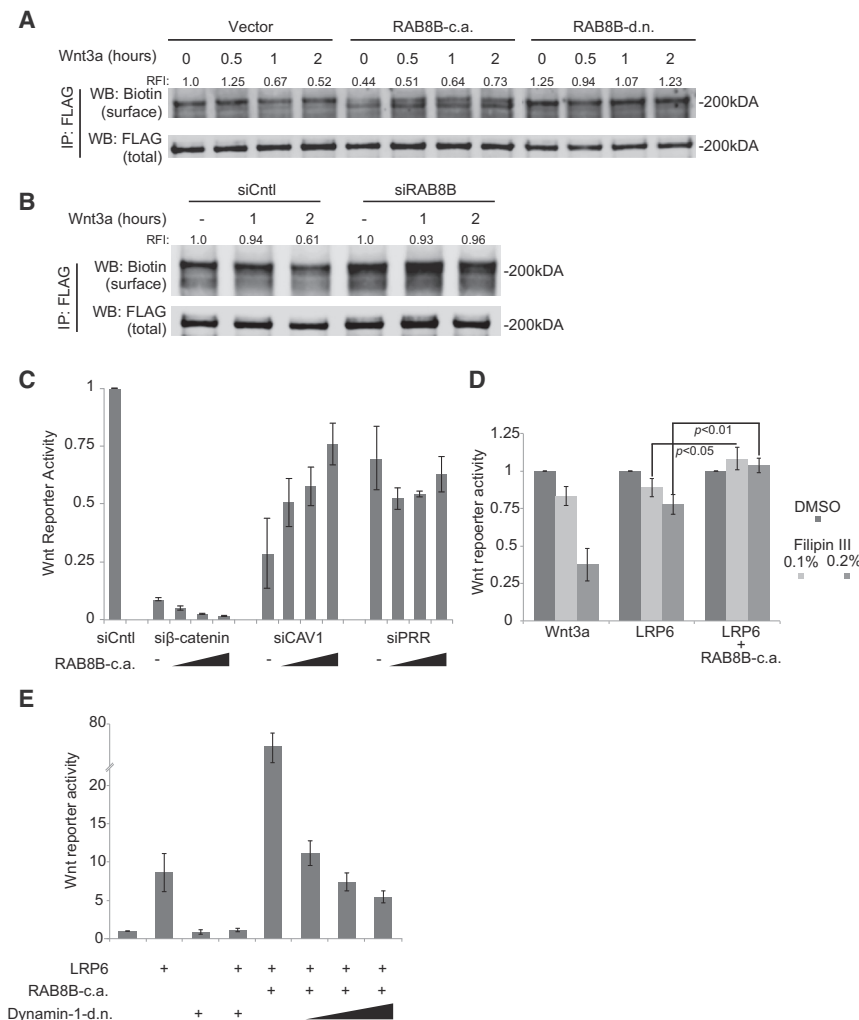WB: FLAG (total) — -200kDA

C — **D** — **E**

Figure 4. RAB8B Promoted Caveolin-Mediated Endocytosis of LRP6

(A) RAB8B-c.a. expression reduced biotinylated FLAG-LRP6 at the plasma membrane both in the presence or absence of Wnt3a, whereas RAB8B-d.n. had the opposite effect, as quantified (normalized to FLAG) by fluorescence immunoblotting (HEK 293T).

(B) RAB8B-depleted cells had higher plasma membrane levels of biotinylated FLAG-LRP6 (normalized to FLAG) in the presence of Wnt3a (HEK 293T).

(C) In the Wnt reporter assay, cells were activated with LRP6 coexpression. RAB8B-c.a. rescued knockdown of Caveolin-1 that was required for internalization, but not PRR that was required for vacuolar acidification (HEK 293T).

(D) Caveolae inhibitor Filipin III reduced Wnt reporter activity that was activated upon Wnt3a or LRP6 coexpression, which could be rescued by RAB8B-c.a. coexpression (HEK 293T).

(E) Dynamin-1 mutant (K44A) abrogated the synergistic phenotype of RAB8B-c.a. in the Wnt reporter assay (HEK293T).

Error bars represent ±SD of three replicates. See also Figure S4.

zation. This finding suggests that RAB8B's activity promotes receptor internalization leading to subsequent endocytosis. Then, we asked if we could also mimic RAB8B-d.n. phenotype by depleting RAB8B in the same assay. RAB8B siRNAs also reduced LRP6 internalization at the plasma membrane underscoring RAB8B's requirement for endocytosis (Figure 4B). CAV1 is required for caveolar invagination and subsequent internalization of LRP6, whereas PRR/ATP6AP2 serves as an adaptor protein between LRP6 and v-ATPase in vacuolar acidification (Cruciat et al., 2010), and knockdown of CAV1 or PRR led to decreased Wnt reporter activity. Expression of RAB8B-c.a. partially rescued the CAV1 but not the PRR RNAi phenotype, suggesting a role for RAB8B in caveolin-dependent internalization of LRP6 (Figure 4C). Filipin III, a small molecule disrupting caveolar microdomains, inhibited Wnt reporter activity in a dose-dependent manner when cells were stimulated with Wnt3a or LRP6 expression. Coexpression of RAB8B-c.a. rescued this inhibitory effect through synergizing with LRP6, supporting its caveolar promoted uptake (Figure 4D). Accordingly, both RAB8B-WT and -c.a. displayed similar patterns and appeared to colocalize with endogenous CAV1, whereas RAB8B-d.n. had a discrete cytoplasmic punctual staining (Figure S4C).

Dynamin GTPase (Dyn) is required for caveolin-mediated endocytosis in the scission of invaginated vesicles from the cell surface, which can be suppressed by expression of a dominant-negative Dyn1 K44A mutant (Ahn et al., 2002). If the observed RAB8B-dependent stimulation of Wnt pathway activity

(Figure S4A), and they also colocalize at the plasma membrane, similarly to LRP6 (Figure S4B). These results further support that RAB8B's regulates signalosome activity, potentially through interacting and promoting local enrichment of its components in the microdomains leading to subsequent vesicular endocytosis.

RAB8B Promotes Caveolin-Mediated Internalization of LRP6

Endocytosis and subsequent trafficking is a key mechanism that regulates receptor-mediated signaling. Wnt ligand binding triggers signalosome formation and concomitant caveolin-dependent endocytosis for downstream signal relay. We therefore hypothesized that RAB8B's effect on LRP6 activity may promote its endocytosis. To test this, we transfected HEK 293T cells with FLAG-LRP6 in the presence of RAB8B-c.a., -d.n., or empty vector and labeled cell-surface proteins using a nonmembrane permeating marker. Wnt3a exposure reduced LRP6 levels at the plasma membrane by promoting its endocytosis with 1–2 hr of exposure (Figure 4A). RAB8B-c.a. readily decreased the amount of LRP6 at the cell surface even in the absence of Wnt3a, whereas RAB8B-d.n. inhibited Wnt3a-induced internali-

was indeed mediated through increased internalization of the receptor complex, interfering with this process should block the effect of RAB8B activity. As predicted, expression of Dyn1 K44A in HEK 293T cells abolished the synergistic stimulation of the Wnt reporter activity by RAB8B-c.a. in a dose-dependent manner (Figure 4E). These results together demonstrate that RAB8B promotes caveolar endocytosis of LRP6 that is required for pathway activation.

RAB8B Is Required for Wnt/β-Catenin Signaling in Zebrafish and *Xenopus*

To test whether the function of RAB8B was also required in vivo for Wnt/β-catenin signaling, we examined its role in zebrafish embryos. Using an in situ probe against zebrafish *rab8b*, we found its earliest expression in the developing brain at early somitogenesis (Figure 5A). Subsequently, *rab8b* transcripts were found widespread in the CNS including regions of known Wnt signaling centers such as the midbrain-hindbrain boundary (MHB) and otic vesicles (OV) (Ladher et al., 2000; Lekven et al., 2001). Cells in these areas were Wnt pathway active as indicated by strong GFP expression in live Tg(7xTCF-XLa.Siam:eGFP)[ia4] transgenic embryos expressing GFP under the control of β-catenin/TCF responsive elements (Moro et al., 2012). Specific knockdown of *rab8b* by ATG or splice site morpholino oligonucleotides resulted in a strong decrease of GFP expression at the MHB and the OV (Figures 5B, S5A, and S5B). *C-myc* (*myca*) is a Wnt target gene expressed in the brain, including the tectum (Thisse and Thisse, 2004). In accordance with Wnt reporter results, we found that expression of *c-myc* in the tectum of *rab8b* morphants was severely reduced (Figure 5B). These results showed that RAB8B's role in Wnt/β-catenin pathway was also required in vivo.

Furthermore, we analyzed RAB8B's requirement for Wnt/β-catenin signaling *in Xenopus* embryos. The injection of two independent antisense morpholino oligonucleotides targeting *rab8b* gave rise to similar phenotypes, corroborating their specificity. Morphant tadpoles displayed smaller heads and eyes, shortened tails, and reduced melanocytes and eye pigmentation (Figure 5C). This phenotype resembled conditions where both Wnt/Planar cell polarity and Wnt/β-catenin signaling were affected as both pathways share components at the receptor level (Buechling et al., 2010; Cruciat et al., 2010). In *Xenopus* Wnt-TOPFlash reporter assays both morpholinos reduced endogenous reporter activity in a dose-dependent manner, comparable to that of LRP6 depletion (Figure 5D). The degree of TOPFlash reporter inhibition correlated with the strength of the developmental phenotypes of the respective morpholinos. Moreover, *rab8b* morpholino-2 completely abrogated ectopic pathway activation upon coinjection of *wnt3a* mRNA mirroring the observations under endogenous Wnt activity (Figure 5E). Taken together, these results show that RAB8B's function is required in vivo, and underscore its role in Wnt/β-catenin signaling during early vertebrate development.

DISCUSSION

Although the Wnt signaling pathway has been studied extensively, it is still poorly understood how caveolin-dependent endocytosis of the Fz-LRP6 receptor complex is mediated upon stimulation with Wnt ligands (reviewed in Niehrs, 2012). Caveolae are stable, flask-shaped, caveolin-1-positive invaginations that are enriched in lipid-raft microdomains containing cholesterol and glycosphingolipids. Wnt stimulation induces binding of LRP6 to caveolin, which is then internalized along with signalosome components. Unlike Wnt ligands, Wnt antagonists, such as Dickkopf (Dkk), remove LRP6 from the lipid rafts inducing its clathrin-dependent endocytosis. Because Wnts and Dkk bind to LRP6 in both lipid-raft and non-lipid-raft fractions of the plasma membrane promoting its endocytosis, it is intriguing to speculate that there are other trafficking factors specifically linking caveolar internalization of the activated receptor complex to MVBs. Here, we provide evidence that RAB8B is required for LRP6 activity and its caveolin-mediated endocytosis.

RAB8B's Function Is Required in Wnt-Receiving Cells at the Receptor Level

More than 60 different Rab proteins have been identified in the human genome with diverse regulatory roles. We identified one of them, RAB8B, as a strong modulator of the canonical Wnt pathway. RNAi-epistasis experiments placed the activity of RAB8B at the level of the receptors in Wnt-receiving cells, which were further supported by perturbation of LRP6 activity and subsequent active β-catenin accumulation in the nucleus. RAB8B does not belong to housekeeping Rabs, such as Rab1/4/5/6/9/11, which are ubiquitously expressed, and whose activities are continuously required (Gurkan et al., 2005). To exclude pleiotropic trafficking roles of RAB8B, we confirmed that RAB8B-RNAi did not reduce the activities in major signaling pathways that also require external stimuli for activation. Unlike RAB8B, depletion of its paralog RAB8A did not change Wnt activity under our experimental conditions, confirming the reported diverse functions of other Rab isoforms (Progida et al., 2010). As the membrane specific domain of RAB8 is less conserved, both proteins might have distinct, as well as overlapping targets.

RAB8B Is Activated by Wnt Ligands, Synergizes, and Interacts with LRP6

The effect of overexpressing different RAB8B forms in cells under different levels of endogenous Wnt signaling activity revealed that RAB8B enhances Wnt signaling together with LRP6 downstream of canonical Wnt ligands. In Wnt-expressing and Wnt-pathway active HCT116 cells, both ectopically expressed wild-type and constitutively active forms of RAB8B could further increase Wnt signaling activity. This effect required the GTPase activity of RAB8B, as the dominant-negative mutant differing in only one amino acid did not show synergistic phenotype. In contrast, in HEK 293T cells, which display low baseline levels of Wnt pathway activity, expression of the wild-type protein had no effect. Yet, once cells were stimulated with Wnt3a treatment or Dvl coexpression, increased expression of RAB8B promoted the pathway activity underlining that LRP6 endocytosis—enhanced by RAB8B activity—is a rate-limiting step under these conditions. These findings indicate that RAB8B's function is required at the level of signal amplification,
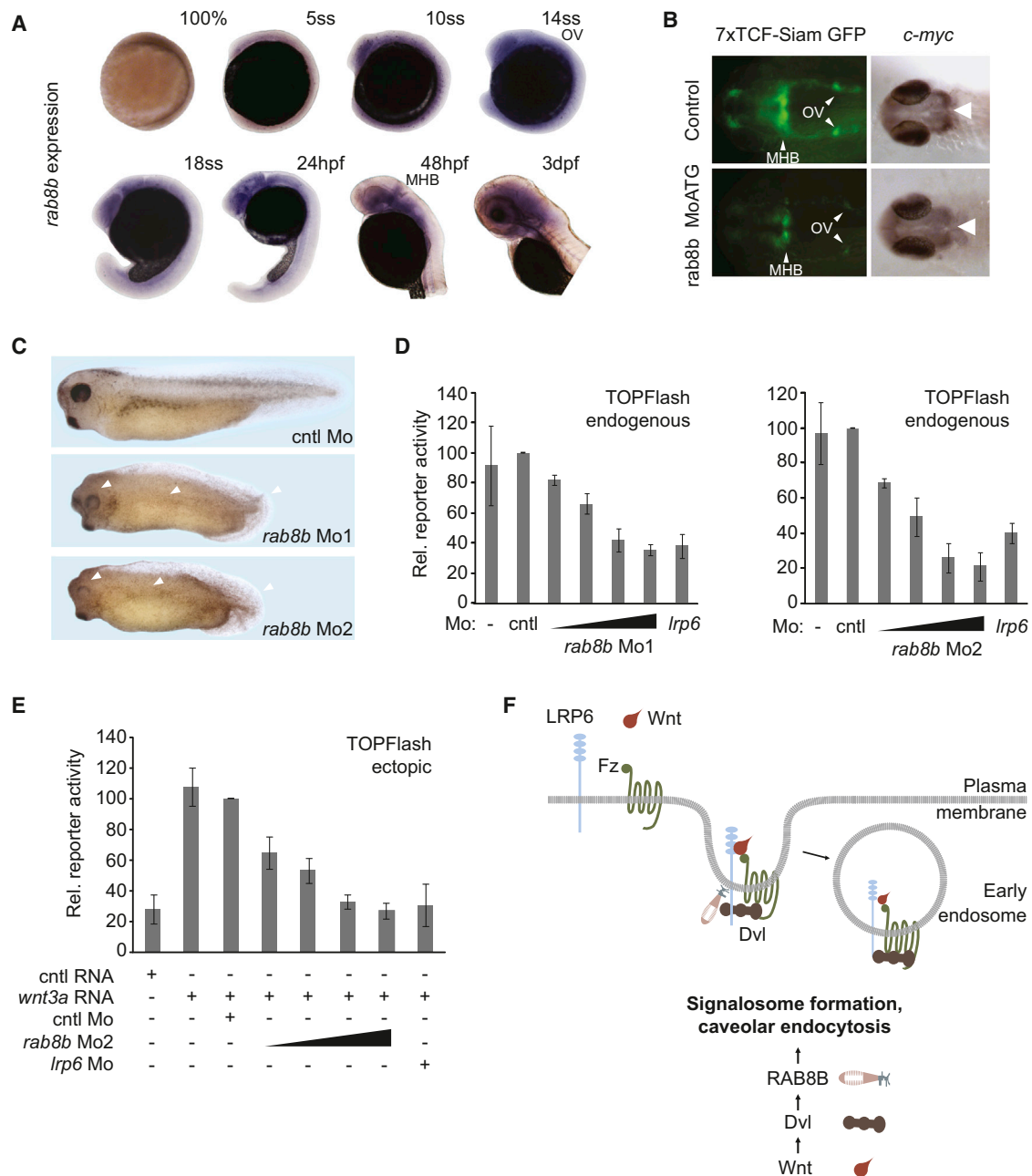
Figure 5. RAB8B Was Required for Wnt/β-Catenin Signaling in Zebrafish and Xenopus

(A) Lateral views of in situ hybridization analysis of *Rab8b* gene expression between 100% of epiboly and 3 days postfertilization (dpf). *Rab8b* is expression is enriched in MHB and OV from early somitogenesis through subsequent organogenesis stages (ss, somite stage).

(B) Dorsal views of 30 hr postfertilization (hpf) embryos focused on the head region. Injection of *rab8b* ATG-morpholino into Tg(7xTCF-XLa.Siam:eGFP)[ia4] transgenic zebrafish expressing GFP upon induction of the synthetic 7XTCF-Siam promoter by β-catenin, resulted in reduced GFP intensity in MHB and OV (n = 49/66), and *c-myc* expression in the tectum (n = 17/27).

(C) *rab8b* morpholino 1 (Mo1) and 2 (Mo2) showed similar Wnt loss-of-function phenotypes in *Xenopus* embryos.

(D and E) Wnt luciferase reporter activity was reduced by *rab8b* Mos in *Xenopus* embryos. Embryos were injected with morpholinos and mRNAs as indicated and luciferase reporter assays were performed at gastrula stage. Relative luciferase activity in embryos injected with control-Mo or control-Mo plus mRNA of the indicated activators.

(F) Model.

Error bars represent ±SD of three replicates. See also Figure S5.

i.e., signalosome complex formation, which requires upstream activation by Wnt ligands.

RAB8B knockdown reduced Wnt reporter activity induced through Dvl1 coexpression but showed no effect with the coexpression of the self-aggregating LRP6Δe1-4. These observations are concordant with a model in which recruitment of Dvl1 to the Wnt-Fz-LRP6 receptor complex activates RAB8B. Dvl1 induced accumulation of RAB8B in large Dvl1 puncta, which are vesicular structures that also contain early endosome marker PI3P. In accordance, Wnt ligands induced interaction of RAB8B with its activator RABIN8. These findings corroborate RAB8B's Wnt-dependent activation and trafficking role. A similar mechanism was proposed to explain how the GTPase Rac1 is activated through LRP5/6, Dvl, $G\alpha_{q/11}\beta_\gamma$, and PI3K (Wu et al., 2008). This model is supported by the observed interactions between RAB8B and LRP6 and also accommodates the synergistic effects of overexpressing both proteins simultaneously.

RAB8B Promotes Caveolin-Dependent Endocytosis of LRP6

Ectopic expression of RAB8B-c.a. reduced cell-surface levels of LRP6, whereas RAB8B-d.n. and RAB8B RNAi had the opposite effect. This could be explained by the lack of signalosome activity/maturation for further trafficking into early endosomes. RAB8B-c.a. rescued the inhibitory effects of both CAV1 depletion and Filipin III treatment on LRP6 internalization and Wnt pathway activity. Importantly, RAB8B activity can be blocked by expression of a dominant-negative form of Dynamin, which is required for vesicle scission from the plasma membrane. These observations point toward a function for RAB8B in caveolae, during an early phase of endocytosis. This hypothesis is further supported by the observations that the WT and c.a. forms of RAB8B showed similar localization patterns with endogenous CAV1 at the plasma membrane, and RAB8B was recruited in PI3P-positive Dvl puncta upon Dvl1 coexpression. TBK1 kinase was identified as a RAB8B interactor in mediating maturation of autophagosomes (Pilli et al., 2012). Because multifunctional TBK1 kinase also interacts and phosphorylates VPS37C, a structural component of ESCRT-I complex (Da et al., 2011), it is tempting to speculate that RAB8B's function may require TBK1 in further trafficking to MVBs. These reports, along with ours, suggest potential endocytic roles of RAB8 proteins are yet to be discovered in different contexts.

RAB8B's Function in Wnt/β-Catenin Pathway Is Required In Vivo

In zebrafish, we found that *rab8b* is expressed ubiquitously in the CNS where Wnt signaling is prominently involved. Moreover, it is markedly enriched in the midbrain-hindbrain boundary and otic vesicles, which are distinct Wnt active domains. This spatial correlation indicates that RAB8B's function is specifically required in Wnt-active regions, and it partially overlaps with that of broadly expressed LRP6 (Chen et al., 2009). In accordance with the cell-based findings, perturbation of RAB8B activity reduced target gene *c-myc* and in vivo reporter protein levels in these regions. Consistent with endogenous *rab8b* expression, posterior regions with Wnt active cells were not affected in the *rab8b* morphants (Figure S5A), indicating Rab8b's function is required in specifically CNS patterning in the zebrafish. However, we did not observed any apparent gross morphological alterations, which is likely due to its temporal expression pattern. *Rab8b* is expressed between 5- and 10-somite stages before which most of the major developmental patterning events have already taken place. In *Xenopus laevis* embryos, *rab8b* mRNA is present as early as stage 2 (Irie and Kuratani, 2011), implying its requirement in development at early stages. *Rab8b* morphants show some aspects of the characteristic Wnt-loss-of function phenotypes, such as loss of eye pigmentation, reduced melanocytes, and shortened tail. (Hassler et al., 2007). Furthermore, ablation of RAB8B function in *Xenopus* embryos reduced TOPFlash reporter and mirrored our findings in zebrafish. These altogether underscored the conserved regulatory role of RAB8B in Wnt signaling during early vertebrate development, which is further supported by the observed synergistic phenotype of *Xenopus* RAB8B in human cells.

Summary

Based on our findings, we suggest the following mechanism of RAB8B in Wnt/β-catenin pathway (Figure 5F): Wnt ligands activate the pathway by binding to Fz-LRP6 receptors and promote their accumulation in caveolae. The Wnt-Fz-LRP6 ternary complex recruits signalosome components, including Dvl, GSK3B, and CK1γ, amplifying signal transduction. During this step, RAB8B is recruited to signalosomes and activated in a Dvl- and Wnt-dependent manner. RAB8B positively regulates signalosome formation and/or maturation and it promotes LRP6 activity leading to subsequent caveolin-mediated endocytosis of the receptor complex.

EXPERIMENTAL PROCEDURES

Cloning

RAB8B ORFs were amplified from cDNAs and cloned into BamHI and XhoI restriction sites of the pCS2+ vector with an N-terminal HA-tag. Constitutively active, dominant-negative, and RNAi-insensitive (ACGATAGAACTAGATGG AAAG > ACCATCGAGCTGGACGGCAAAA) RAB8B forms were generated by PCR-mediated mutagenesis as described (Tomic et al., 1990; Zhang et al., 2007). EGFP-RAB8B fusion protein was generated using XhoI and BamHI restriction sites in the pEGFP-C1 vector (BD Biosciences, Clontech Laboratories).

PAGE-purified, 5'-termini-phosphorylated, sense and antisense long single oligos containing 6xKD and 6xTOPFlash reporter elements were synthesized (Sigma), annealed, and cloned into XhoI and HindIII restriction sites of pGL4.23 and pGL4.26 luciferase vectors (Promega).

Oligonucleotide sequences for the cloning of Wnt reporters are as follows: 6xTOPFlash sense, TCGAGAAGATCAAAGGGGGTAAGATCAAAGGGGGTAA GATCAAAGGGGGCCCCCTTTGATCTTACCCCCTTTGATCTTACCCCCTTTG ATCTTA; 6xTOPFlash antisense, AGCTTAAGATCAAAGGGGGTAAGATCAA AGGGGGTAAGATCAAAGGGGGCCCCCTTTGATCTTACCCCCTTTGATCTTA CCCCCTTTGATCTC; 6xKD sense, TCGAGATCTTCAAAGGGCTAATCTTCA AAGGGCTAATCTTCAAAGGGCTAACCGGTAGCCCTTTGAAGATTAGCCCTTT GAAGATTAGCCCTTTGAAGATA; 6xKD antisense, AGCTTATCTTCAAAGGG CTAATCTTCAAAGGGCTAATCTTCAAAGGGCTACGGCTAGCCCTTTGAAGA TTAGCCCTTTGAAGATTAGCCCTTTGAAGATC.

Cell-Culture and Nucleic Acid Transfections

HEK 293T cells and HeLa cells were maintained in DMEM, HCT116 cells (ATCC-CCL-247) was maintained in McCoy's 5A medium at 37°C in humidified atmosphere with 5%CO₂, with 10% fetal bovine serum (Biochrom) and 50 μg/ml penicillin/streptomycin. Transient transfections were performed

according to supplier instructions (TransIT-LT1-Mirus, RNAiMax-Invitrogen). siRNAs were used at a final concentration of 12.5 nM for Ambion and 50 nM for Dharmacon, respectively.

Wnt reporter assays were performed in 384-well assay plates, with 5 ng of Wnt reporter firefly luciferase and 40 ng of constitutively active renilla luciferase containing endogenous β-actin promoter (Nickles et al., 2012). Firefly to renilla luciferase ratio was calculated for each well and normalized to siCntl-transfected or mock-treated (in the absence of RNAi) cells. Epistasis experiments were performed with 1 ng mouse Wnt3a, 5 ng of human LRP6, 5 ng of human Dvl1, 5 ng of human LRP6Δe1-4, or 1 ng of Xenopus β-catenin. Wnt3a conditioned media was prepared from Mouse-L cells (ATCC-CRL-2647) as described by the supplier. Thirty microliters of conditioned media or recombinant Wnt3a (50 ng/ml) was added to cells 24 hr before readout. Other reporter assays were performed as previously described (Cruciat et al., 2010). Recombinant Wnt3a, FGF8, BMP4, and TGF-β were purchased from Peprotech, TNF-α and interleukin (IL)-6 were purchased from Invitrogen, and Filipin III (F4767) was purchased from Sigma.

RNAi screening was performed with an Ambion SilencerSelect RNAi Library using three single siRNAs per gene. After 72 hr, 50 μl of 8.10^{-5} M Calcein-AM (Sigma) in PBS was added to cells and further incubated for an additional hour. Calcein fluorescence (ex/em: 495/515) and firefly luciferase activities were measured with the multipurpose plate reader (Mithras LB940, Berthold Technologies). Raw data were analyzed with cellHTS2 R-Bioconductor package, in which values of firefly normalized to Calcein (Boutros et al., 2006; Gilbert et al., 2011). Cellular viability measurement was performed with CellTiter-Glo reagent according to supplier's instructions (Promega).

siRNA sense strand sequences were as follows: β-catenin (CUGUUG GAUUGAUUCGAAA, Ambion-s438); LRP6 (GGCUACAAAUGUUCAUCGA, Ambion-s8291); UBC (GUGAAGACCCUGACUGGUA, Ambion-s14559); RAB8B #1,2,3 (GAAAGAUUCCGAACAAUCA, CGAUAGAACUAGAUGGAAA, GAAUGAUCCUGGGUAACAA, Ambion-s28633-4-5); RAB8A (GAAUUAAA CUGCAGAUAUG, GAACAAGUGUGAUGUGAAU, GAACUGGAUUCGCAA CAUU, GAAGACCUGUGUCCUGUUC, Dharmacon Pool, MU-003905-00); APC (GGAUCUGUAUCAAGCCGUU, Ambion-s1433); PRR (GGACUAUCCUU GAGGCAAA, GGGAACGAGUUUAGUAUAU, GAGUGUAUAUGGUAGGGAA, CAGGCAGUGUCAUUUCGUA, Dharmacon Pool, MU-013647-00); CAV1 (CUAAACACCUCAACGAUGA, GCAGUUGUACCAUGCAUUA, AUUAAGAGC UUCCUGAUUG, GCAAAUACGUAGACUCGGA, Dharmacon Pool, MU-003467-01); DVL1 (GCGAGUUCUUCGUGGACAU, CGACCAAGGCCUAUAC AGU, CGGCACACGGUCAACAAGA, GGGAGUCAGCAGAGUGAAG, Dharmacon Pool, MU-004068-01).

Quantitative RT-PCR

Quantitative RT-PCR assay was performed in 384-well format (LightCycler 480 System, Roche) using the UPL Probe library and LightCycler Master Mix (Roche). QPCR primers were designed using Roche Universal Probe Library Primer Design Portal. Analysis of the qPCR data was performed using ACTB and GAPDH genes as normalization controls (Pfaffl, 2001).

Primer sequences and UPL probe numbers were as follows: ACTB UPL#11 (F-ATTGGCAATGAGCGGTTC, R-TGAAGGTAGTTTCGTGGATGC), GAPDH UPL#60 (F-AGCCACATCGCTCAGACAC, R-GCCCAATACGACCAAATCC), AXIN2 UPL#88 (F-AGAGCAGCTCAGCAAAAAGG, R-CCTTCATACATCGG GAGCAC), SMAD7 UPL#6 (F-CGATGGATTTTCTCAAACCAA, R-AGGGGCC AGATAATTCGTTC), RAB8B UPL#16 (F-GACTCGGGGGGTAGGCAAG, R-TT TCTTTCCATCTAGTTCTATCGTTCT), RAB8A UPL#54 (F-AAAAGCTGG CCCTCGACTAT, R-CTGGCGAGAGTGAAAAATGC), Dvl1 UPL#63 (F-AAGA ACGTGCTCAGCAACC, R-AGCTTGGCATTGTCATCAAA), LRP6 UPL#79 (F-AGAACGCGAGAAGGGAAGAT, R-TGTTTGCATAAAGCAACAAAGG).

Immunoassays

In immunoblot assays, cell lysates were prepared with M-Per mammalian protein extraction buffer (Pierce) containing protease inhibitor tablet (Roche) and phosphatase inhibitor cocktails (Sigma, II and III) and were loaded with reducing buffer (Roti-Load 1) in NuPage BT 4%–12% Gels (Invitrogen). Blot images were acquired and quantified with LICOR Odyssey FC imaging system using fluorescent secondary antibodies.

For immunoprecipitation assays, anti-FLAG M2 agarose (Sigma, A2220) or anti-HA agarose (Sigma, A2095) were used in at 4°C with IP lysis buffer (30 mM Tris-HCl [pH 7.5], 150 mM NaCl, 10% glycerol), freshly supplemented with protease inhibitor tablet (Roche), 1% Triton X-100, 1 mM EDTA, and phosphatase inhibitor cocktails (Sigma, II and III). For the LRP6 internalization assay, cells were incubated on ice for 5 min to completely block endocytosis and incubated with ice-cold PBS containing 0.5 mg/ml impermeable, noncleavable EZ-Link Sulfo-NHS-LC-LC-Biotin (Pierce, 21338) for 45 min on ice. Cells were then washed with 3× ice-cold PBS containing 100 mM glycine amino acid to quench biotinylation. Surface LRP6 (Biotin) intensities were normalized to corresponding total LRP6 (FLAG) intensities in each sample.

For immunofluorescence assays, cells seeded on coverslips were fixed with 4% PFA-PBS for 30 min followed by permeabilization with 0.3% Triton X-100-PBS for 15 min and blocked with 5% goat serum (Dako X090710) for 1 hr, at room temperature. Cells were incubated with blocking buffer containing 5% goat serum (Dako X090710), 0.3% Triton X-100 in PBS for 1 hr. Antibody incubations were performed overnight at 4°C using antibody dilution buffer containing 1% BSA, 0.3% Triton X-100 in PBS. Microscopy images were taken with Leica SP5 system using the 63× oil objective, and raw channel images were analyzed and merged with ImageJ (Abramoff et al., 2004) and directly imported to Adobe Illustrator. Correlation of colocalization was analyzed with ImageJ and JACoP plugin (Bolte and Cordelières, 2006; Schneider et al., 2012).

Antibodies

In immunoblot experiments, primary antibodies were mouse anti-total β-catenin (1:2,000, BD Biosciences, 610154), mouse anti-active β-catenin (1:1,000, Clone 8E7, Millipore 05-665), rabbit anti-total LRP6 (1:1,000, Cell Signaling Technology, C5C7, 2560), rabbit anti-S1490 LRP6 (1:1,000, Cell Signal, 2568), rabbit anti-T1479 LRP6 (1:1,000, custom made, Davidson et al., 2005), mouse anti-FLAG (1:2,000, Sigma, M2 Clone, F1804), rabbit-anti FLAG (1:2,000, Sigma, F7425), mouse-anti-FLAG-HRP (1:5,000, Sigma, A8592), rabbit anti-RABIN8 (1:1,000, Proteintech, 12321-1-AP), mouse anti-HA (1:2,000, Cell Signal, 6E2, 2367), rabbit-HA (1:2,000, Sigma, H6908), mouse anti-β-actin (1:10,000, Abcam, AC15, 6276), mouse anti-biotin (1:1,000, Dianova, DLN-06043), anti-mouse HRP (1:20,000, GE Healthcare, NA931), anti-rabbit-HRP (1:20,000, GE Healthcare, NA934), anti-mouse-HRP (1:10,000, TrueBLOT ULTRA, eBioscience, 18-8817-33), anti-rabbit-HRP (1:10,000, TrueBLOT ULTRA, eBioscience, 18-8816-33), and for Li-Cor Odyssey FC imaging system, anti-mouse DyLight 680 Conjugate (1:10,000, Thermo Fisher Scientific, 35518), anti-rabbit DyLight 800 Conjugate (1:10,000, Thermo Fisher Scientific, 35571).

In immunofluorescence experiments, antibodies were mouse anti-FLAG M2 (1:500, Sigma-Aldrich, F1804), mouse anti-Dvl1 (1:500, Santa Cruz Biotechnology, sc-8025), rat anti-HA-Fluorescein-High affinity (1:500, Roche, 3F10), rabbit anti-Caveolin-1 (1:500, Cell Signaling Technology, 3267), goat anti-mouse Alexa Fluor 594 conjugated (1:1000, Invitrogen, A11005), goat anti-rabbit Alexa Fluor 633 conjugated (1:1,000, Invitrogen, A21071).

In immunoprecipitations, anti-HA-conjugated agarose (Sigma-Aldrich, A2095), anti-FLAG-conjugated agarose (Sigma-Aldrich, A2220), rabbit anti-Nanog (as isotype control, Cell Signaling Technology, D73G4, 4903), and rabbit anti-total LRP6 (1:1000, Cell Signaling Technology, C5C7, 2560) were used.

In Vivo Assays

In Xenopus mRNA and Morpholino injections, the antisense Morpholino (Mo) oligonucleotides were used as follows if not described otherwise (per embryo): 5 ng, 10 ng, 20 ng, and 40 ng rab8b Mo1 (GGTAGTCGTAAGTCTTCGCC ATCTT) and 10 ng, 20 ng, 40 ng, and 60 ng rab8b Mo2 (AAGTCTTCGCC ATCTTTAGTCCTCC). The Wnt3a mRNA dose for injections was 4 pg per embryo. Equal amounts of total Mo/RNA were injected by adjustment with the standard control Mo (Gene Tools) or PPL RNA, where necessary.

In zebrafish embryo injections, 2 nl of ATG (MoATG, 0.2 mM, TTCGCCAT ATTTTCTTGTTTCTCCC) or splicing (MoSpl, 0.8 mM, CTCTAGTGTGAAACT GACCTATGGT) morpholino antisense oligonucleotides (Gene Tools) were injected at one-cell stage embryos. Morpholino oligonucleotides were

designed and synthesized by GeneTools. Injection experiments were repeated at least three times.

In fish stock maintenance, AB × TL wild-type and Tg(7xTCF-XLa.Siam:eGFP)[ia4] transgenic lines were preserved and bred according to standard procedures (Westerfield, 1995). To inhibit pigmentation, the embryos were raised in 0.2 mM 1-phenyl-2 thiourea.

Digoxigenin RNA Labeling Kit (Roche) and hybridizations were performed as described (Macdonald et al., 1994). Splicing morpholino specificity was confirmed with RT-PCR at 30 hpf. GFP fluorescence was acquired at 30 hpf using the Leica MZ16F system.

For cloning of *rab8b* cDNA, total RNA was isolated from 30 hpf embryos using QIAGEN RNA Extraction Kit. RT-PCR reactions were performed using SuperScript III Reverse Transcriptase Kit (Invitrogen). The *rab8b* cDNA was amplified using the following primers: *rab8b*_in situ_forward (5′-GCTGC TCATCGGAGACA-3′), *rab8b*_in situ_reverse (5′-TAGCGACTGACGAGCC-3′). PCR conditions were as follows: 29 cycles: 30 s at 95°C, 60 s at 56°C, 110 s at 72°C. The resulting cDNA fragment was cloned into a pCRII-TOPO vector (Invitrogen) and verified by sequencing. *Rab8b* splicing morpholino specificity was investigated at 30 hpf by RT-PCR using primers binding upstream to the splicing morpholino binding site in exon 1 and downstream in intron 1. The PCR product was verified with HpaI digestion and sequencing. *Wnt7aa* and *runx1t1* transcript levels were used as controls. Primer sequences and PCR reaction conditions were: *rab8b* splicing primer forward (5′-GCTGCTCATCG GAGACA-3′), *rab8b* splicing primer reverse (5′-TCACCACTAAACGGGA CT-3′), *wnt7aa* primer forward (5′-GCCGCTGGATTTTTCACAT-3′), *wnt7aa* primer reverse (5′-TGTGTACACTTCTGTCCGTTCACT-3′), *runx1t1* primer forward (5′-CTCACCTGCTGATGTGA-3′), and *runx1t1* primer reverse (5′-GCAACTCACTGGGGTCA-3′); 35 cycles: 60 s at 95°C, 60 s at 60°C, 120 s at 72°C.

In in situ hybridization experiments, images were acquired using Leica DM6000B system. Raw images were montaged with Fiji (Schindelin et al., 2012) and directly incorporated into Adobe Illustrator.

All experiments on living *Xenopus* and zebrafish organisms were performed in accordance with state and regional board guidelines (Az. 35-9185.81/G-139/08 and 35-9185.64).

Statistics

Results are given as ±SD) of replicates. Statistical analyses were performed with Excel (Microsoft) applying two-tailed t test, as appropriate. p values < 0.05 were considered as significant.

SUPPLEMENTAL INFORMATION

Supplemental Information includes five figures and can be found with this article online at http://dx.doi.org/10.1016/j.celrep.2013.08.008.

REFERENCES

Abramoff, M.D., Magalhaes, P.J., and Ram, S.J. (2004). Image Processing with ImageJ. Biophotonics International *11*, 36–42.

Ahn, S., Kim, J., Lucaveche, C.L., Reedy, M.C., Luttrell, L.M., Lefkowitz, R.J., and Daaka, Y. (2002). Src-dependent tyrosine phosphorylation regulates dynamin self-assembly and ligand-induced endocytosis of the epidermal growth factor receptor. J. Biol. Chem. *277*, 26642–26651.

Behrens, J., von Kries, J.P., Kühl, M., Bruhn, L., Wedlich, D., Grosschedl, R., and Birchmeier, W. (1996). Functional interaction of beta-catenin with the transcription factor LEF-1. Nature *382*, 638–642.

Bilic, J., Huang, Y.-L., Davidson, G., Zimmermann, T., Cruciat, C.-M., Bienz, M., and Niehrs, C. (2007). Wnt induces LRP6 signalosomes and promotes dishevelled-dependent LRP6 phosphorylation. Science *316*, 1619–1622.

Bolte, S., and Cordelières, F.P. (2006). A guided tour into subcellular colocalization analysis in light microscopy. J. Microsc. *224*, 213–232.

Boutros, M., Brás, L.P., and Huber, W. (2006). Analysis of cell-based RNAi screens. Genome Biol. *7*, R66.

Buechling, T., Bartscherer, K., Ohkawara, B., Chaudhary, V., Spirohn, K., Niehrs, C., and Boutros, M. (2010). Wnt/Frizzled signaling requires dPRR, the Drosophila homolog of the prorenin receptor. Curr. Biol. *20*, 1263–1268.

Chen, M., Philipp, M., Wang, J., Premont, R.T., Garrison, T.R., Caron, M.G., Lefkowitz, R.J., and Chen, W. (2009). G Protein-coupled receptor kinases phosphorylate LRP6 in the Wnt pathway. J. Biol. Chem. *284*, 35040–35048.

Cruciat, C.M., Ohkawara, B., Acebron, S.P., Karaulanov, E., Reinhard, C., Ingelfinger, D., Boutros, M., and Niehrs, C. (2010). Requirement of prorenin receptor and vacuolar H+-ATPase-mediated acidification for Wnt signaling. Science *327*, 459–463.

Da, Q., Yang, X., Xu, Y., Gao, G., Cheng, G., and Tang, H. (2011). TANK-binding kinase 1 attenuates PTAP-dependent retroviral budding through targeting endosomal sorting complex required for transport-I. J. Immunol. *186*, 3023–3030.

Davidson, G., Wu, W., Shen, J., Bilic, J., Fenger, U., Stannek, P., Glinka, A., and Niehrs, C. (2005). Casein kinase 1 gamma couples Wnt receptor activation to cytoplasmic signal transduction. Nature *438*, 867–872.

Emery, G., Hutterer, A., Berdnik, D., Mayer, B., Wirtz-Peitz, F., Gaitan, M.G., and Knoblich, J.A. (2005). Asymmetric Rab 11 endosomes regulate delta recycling and specify cell fate in the Drosophila nervous system. Cell *122*, 763–773.

Evans, T.M., Ferguson, C., Wainwright, B.J., Parton, R.G., and Wicking, C. (2003). Rab23, a negative regulator of hedgehog signaling, localizes to the plasma membrane and the endocytic pathway. Traffic *4*, 869–884.

Gilbert, D.F., Erdmann, G., Zhang, X., Fritzsche, A., Demir, K., Jaedicke, A., Muehlenberg, K., Wanker, E.E., and Boutros, M. (2011). A novel multiplex cell viability assay for high-throughput RNAi screening. PLoS ONE *6*, e28338.

Gurkan, C., Lapp, H., Alory, C., Su, A.I., Hogenesch, J.B., and Balch, W.E. (2005). Large-scale profiling of Rab GTPase trafficking networks: the membrome. Mol. Biol. Cell *16*, 3847–3864.

Hassler, C., Cruciat, C.M., Huang, Y.L., Kuriyama, S., Mayor, R., and Niehrs, C. (2007). Kremen is required for neural crest induction in Xenopus and promotes LRP6-mediated Wnt signaling. Development *134*, 4255–4263.

Hattula, K., Furuhjelm, J., Arffman, A., and Peränen, J. (2002). A Rab8-specific GDP/GTP exchange factor is involved in actin remodeling and polarized membrane transport. Mol. Biol. Cell *13*, 3268–3280.

Irie, N., and Kuratani, S. (2011). Comparative transcriptome analysis reveals vertebrate phylotypic period during organogenesis. Nature communications *2*, 248.

Klaus, A., and Birchmeier, W. (2008). Wnt signalling and its impact on development and cancer. Nat. Rev. Cancer *8*, 387–398.

Ladher, R.K., Anakwe, K.U., Gurney, A.L., Schoenwolf, G.C., and Francis-West, P.H. (2000). Identification of synergistic signals initiating inner ear development. Science *290*, 1965–1967.

Lekven, A.C., Thorpe, C.J., Waxman, J.S., and Moon, R.T. (2001). Zebrafish wnt8 encodes two wnt8 proteins on a bicistronic transcript and is required for mesoderm and neurectoderm patterning. Dev. Cell *1*, 103–114.

MacDonald, B.T., Tamai, K., and He, X. (2009). Wnt/beta-catenin signaling: components, mechanisms, and diseases. Dev. Cell *17*, 9–26.

Macdonald, R., Xu, Q., Barth, K.A., Mikkola, I., Holder, N., Fjose, A., Krauss, S., and Wilson, S.W. (1994). Regulatory gene expression boundaries demarcate

sites of neuronal differentiation in the embryonic zebrafish forebrain. Neuron *13*, 1039–1053.

Miaczynska, M., Christoforidis, S., Giner, A., Shevchenko, A., Uttenweiler-Joseph, S., Habermann, B., Wilm, M., Parton, R.G., and Zerial, M. (2004). APPL proteins link Rab5 to nuclear signal transduction via an endosomal compartment. Cell *116*, 445–456.

Moro, E., Ozhan-Kizil, G., Mongera, A., Beis, D., Wierzbicki, C., Young, R.M., Bournele, D., Domenichini, A., Valdivia, L.E., Lum, L., et al. (2012). In vivo Wnt signaling tracing through a transgenic biosensor fish reveals novel activity domains. Dev. Biol. *366*, 327–340.

Nickles, D., Falschlehner, C., Metzig, M., and Boutros, M. (2012). A genome-wide RNAi screen identifies CASP4 as a factor required for TNF-alpha signaling. Mol. Cell. Biol. *32*, 3372–3381.

Niehrs, C. (2012). The complex world of WNT receptor signalling. Nat. Rev. Mol. Cell Biol *13*, 767–779.

Pfaffl, M.W. (2001). A new mathematical model for relative quantification in real-time RT-PCR. Nucleic Acids Res. *29*, e45.

Pilli, M., Arko-Mensah, J., Ponpuak, M., Roberts, E., Master, S., Mandell, M.A., Dupont, N., Ornatowski, W., Jiang, S., Bradfute, S.B., et al. (2012). TBK-1 promotes autophagy-mediated antimicrobial defense by controlling autophagosome maturation. Immunity *37*, 223–234.

Progida, C., Cogli, L., Piro, F., De Luca, A., Bakke, O., and Bucci, C. (2010). Rab7b controls trafficking from endosomes to the TGN. J. Cell Sci. *123*, 1480–1491.

Sakane, H., Yamamoto, H., and Kikuchi, A. (2010). LRP6 is internalized by Dkk1 to suppress its phosphorylation in the lipid raft and is recycled for reuse. J. Cell Sci. *123*, 360–368.

Schindelin, J., Arganda-Carreras, I., Frise, E., Kaynig, V., Longair, M., Pietzsch, T., Preibisch, S., Rueden, C., Saalfeld, S., Schmid, B., et al. (2012). Fiji: an open-source platform for biological-image analysis. Nat. Methods *9*, 676–682.

Schneider, C.A., Rasband, W.S., and Eliceiri, K.W. (2012). NIH Image to ImageJ: 25 years of image analysis. Nat. Methods *9*, 671–675.

Stenmark, H. (2009). Rab GTPases as coordinators of vesicle traffic. Nat. Rev. Mol. Cell Biol. *10*, 513–525.

Taelman, V.F., Dobrowolski, R., Plouhinec, J.-L., Fuentealba, L.C., Vorwald, P.P., Gumper, I., Sabatini, D.D., and De Robertis, E.M. (2010). Wnt signaling requires sequestration of glycogen synthase kinase 3 inside multivesicular endosomes. Cell *143*, 1136–1148.

Thisse, B., and Thisse, C. (2004). Fast Release Clones: A High Throughput Expression Analysis. ZFIN Direct Data Submission (http://zfin.org).

Tomic, M., Sunjevaric, I., Savtchenko, E.S., and Blumenberg, M. (1990). A rapid and simple method for introducing specific mutations into any position of DNA leaving all other positions unaltered. Nucleic Acids Res. *18*, 1656.

Westerfield, M. (1995). The Zebrafish Book. A Guide for the Laboratory Use of Zebrafish (*Danio rerio*) (Eugene, OR: University of Oregon Press).

Wu, X., Tu, X., Joeng, K.S., Hilton, M.J., Williams, D.A., and Long, F. (2008). Rac1 activation controls nuclear localization of β-catenin during canonical Wnt signaling. Cell *133*, 340–353.

Yamamoto, H., Komekado, H., and Kikuchi, A. (2006). Caveolin is necessary for Wnt-3a-dependent internalization of LRP6 and accumulation of beta-catenin. Dev. Cell *11*, 213–223.

Zeng, X., Tamai, K., Doble, B., Li, S., Huang, H., Habas, R., Okamura, H., Woodgett, J., and He, X. (2005). A dual-kinase mechanism for Wnt co-receptor phosphorylation and activation. Nature *438*, 873–877.

Zhang, J., Schulze, K.L., Hiesinger, P.R., Suyama, K., Wang, S., Fish, M., Acar, M., Hoskins, R.A., Bellen, H.J., and Scott, M.P. (2007). Thirty-one flavors of Drosophila rab proteins. Genetics *176*, 1307–1322.